Article

NANOMATERIALS AND NANOTECHNOLOGY

Nanomaterials and Nanotechnology
Volume 9: 1–7

DOI: 10.1177/1847980419840858
journals.sagepub.com/home/nax
SAGE

Enhanced mechanical properties of multiwalled carbon nanotubes/ thermoplastic polyurethane nanocomposites

P Kalakonda[1,2], S Banne[3], and PB Kalakonda[4]

Abstract

Carbon nanotubes are considered to be ideal candidates for improving the mechanical properties of polymer nanocomposite scaffolds due to their higher surface area, mechanical properties of three-dimensional isotropic structure, and physical properties. In this study, we showed the improved mechanical properties prepared by backfilling of preformed hydrogels and aerogels of individually dispersed multiwalled carbon nanotubes (MWCNTs-Baytubes) and thermoplastic polyurethane. Here, we used the solution-based fabrication method to prepare the composite scaffold and observed an improvement in tensile modulus about 200-fold over that of pristine polymer at 19 wt% MWCNT loading. Further, we tested the thermal properties of composite scaffolds and observed that the nanotube networks suppress the mobility of polymer chains, the composite scaffold samples were thermally stable well above their decomposition temperatures that extend the mechanical integrity of a polymer well above its polymer melting point. The improved mechanical properties of the composite scaffold might be useful in smart material industry.

Keywords

Polymer nanocomposites, carbon nanotubes, elastic modulus and mechanical integrity

Date received: 9 February 2018; accepted: 21 February 2019

Topic Area: Polymer Nanocomposites and Nanostructured Materials
Topic Editor: Emanuel Ionescu
Associate Editor: Emanuel Ionescu

Introduction

Nanotube polymer composite scaffold has been studied for many industrial applications such as electronic packing, shielding, and storage capacitors.[1–13] Recently, a significant improvement in the mechanical properties was also observed in the composites scaffold.[14] However, there is a big challenge to fabricate the composite scaffold beyond certain higher loading of nanofiller composition due to possible aggregation. Consequently, higher aspect ratio nanofillers are good for larger reinforcement. Carbon nanotubes (CNTs) are the best choice in this regard due to their high aspect ratio and large interfacial area.[15,16] Additionally, the surfaces of nanotubes can be functionalized easily

[1] Department of Materials Science and Engineering, Carnegie Mellon University, Pittsburgh, PA, USA
[2] Division of Physical Sciences and Engineering, King Abdullah University of Science and Technology (KAUST), Thuwal, Kingdom of Saudi Arabia
[3] Department of Materials Science and Metallurgical Engineering, Maulana Azad National Institute of Technology (MANIT), Bhopal, Madhya Pradesh, India
[4] School of Pharmaceutical Sciences and Innovative Drug Research Centre, Chongqing University, Chongqing, People's Republic of China

Corresponding author:
P Kalakonda, Department of Materials Science and Engineering, Carnegie Mellon University, Pittsburgh, PA 15213, USA..
Email: parvathalu.k@gmail.com

and prepared to interact with suitable polymers through the use of suitable coupling agents.[17]

However, there is a big challenge in handling of CNTs, such as aggregation that leads to a nonuniform dispersion and poor interfacial interaction between the nanotubes and the polymer matrix. The nanotubes aggregate easily with a polymer in simple mixing process due to van der Waals attraction between the nanotubes and the polymer matrix. Recently, loading of 1–20 wt% of CNTs into polymers, the most widely used fabrication method, leads to 40–800% strengthening in modulus.[18–20] This poor reinforcement has been attributed due to lower aspect ratio, slippage, and bundling of nanotubes at their atomically smooth surfaces. The fictionalization method is one of the methods through which we can overcome the aggregation, but their intrinsic properties such as electrical and mechanical properties are reduced. To achieve homogeneous dispersion, it is necessary to overcome the aggregation issue in polymers without covalent functionalization and fabricate porous networks of nanotubes backfilled with the polymer matrix. These porous nanotube networks are fabricated via chemical vapor deposition method (CVD), and they contain impurities from synthesis that cannot be removed without damaging the scaffold. They also offer well-controlled size, shape, and pore size as well as reduced control over properties of the constituent nanotubes. Fabrication of backfilling networks has yielded only 100–600% and 60–100% enhancement in E and ultimate tensile strength (UTS), at the loading of 1.5–60 vol% CNTs. This would be possibly due to nanotubes bundle during polymer infiltration fabrication process and have poor interfacial adhesion with polymers.[21,22]

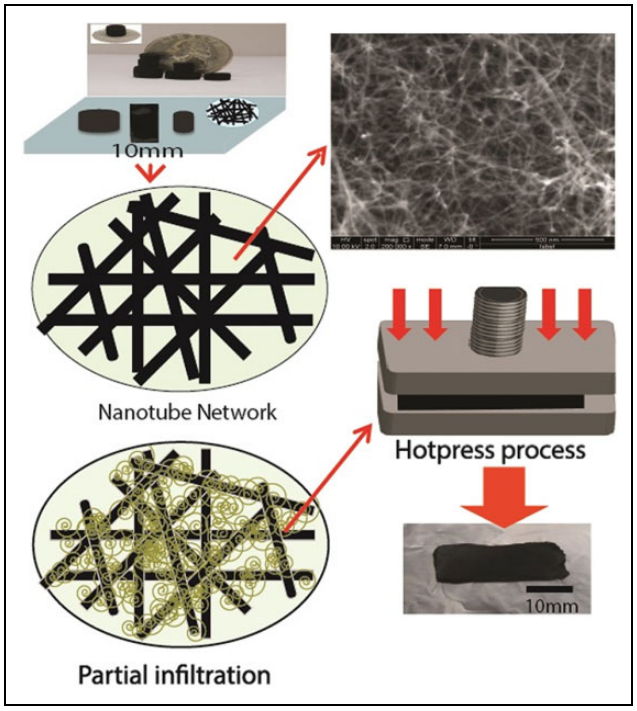

Figure 1. A schematic of the fabrication steps of nanotube polymer composites.

Experimental methods

Materials and sample preparation

A schematic representation of our composite fabrication method is shown in Figure 1. The polymer used in this work is a commercial-grade elastomeric random of thermoplastic polyurethane family (TPU; Texin Sun-3006HF, Bayer Materials, Pittsburg, Pennsylvania, USA) and is composed of hard and soft segments (HS and SS, respectively). This class of polymers is often utilized as a polymer matrix in nanocomposite studies because it has many industrial applications and simple processing. The aliphatic hard segments of TPU are incompatible with soft segments and phase segregate into amorphous or crystalline domains within a network of soft segments. The composition and the hierarchical structures formed by both soft and hard segments indicate the thermomechanical responses of TPU: the hard segments typically influence the modulus and strength, while the soft segments provide stretchability. The TPU used here has approximately 62 wt% of soft segments with the rest being hard segments. The hard segments either do not crystalize or form small crystallized domains that have a melting temperature ($T_{m\ HS}$) of approximately 60°C. Further, the glass-transition temperature of the hard segments ($T_{g\ HS}$) is nearly 30°C and the soft segments are rubbery at room temperature with a $T_{g\ SS}$ of nearly −45°C. The MWCNTs (Baytubes C150P, purity ∼95%, mean diameter of 13–16 nm, and the average length of 1–4 μm) used in this work were purchased from Bayer Material Science.

We have used a solution fabrication method with MWCNTs in hydrogel and aerogel-forms concentration.[23–32] The porous network is stood together primarily via van der Waals interactions at discrete nanotube crossover linking points.[33–38] The nanotubes are dispersed individually within scaffolds and randomly oriented for effective load transfer from polymers to nanofillers. Pore diameters of nanotube network 10–20 nm allow for easy infiltration of polymers. We have partially backfilled the scaffolds with the polymer by soaking them in a polymer solution of concentration 1–6 wt% for 5–10 h at 50°C. By adjusting the polymer solution concentration and soaking time, we have tuned the final nanotube wt% in the composites. At the backfilling temperature, the polymer is in a rubbery state, less viscous and facilitated easy polymer infiltration into the nanotube network. We then evaporated the solvent, annealed the composites under vacuum at 150°C for 12 h and removed all voids by hot-pressing method at 130°C for 10–15 min. The composite scaffolds were used for all measurements in a rectangular shape with an average thickness of 150–200 μm. These composites

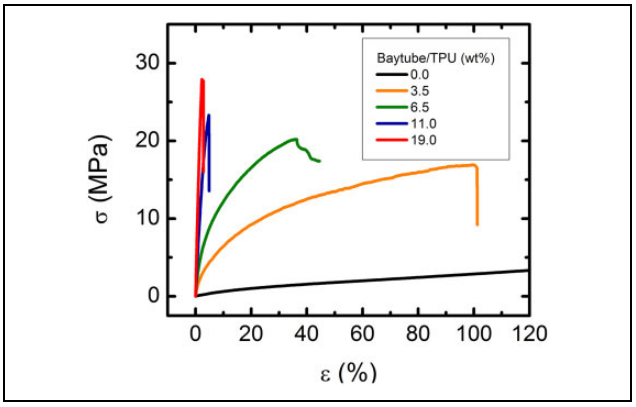

Figure 2. The tensile stress versus strain curves of TPU polymer and composites with various Baytube concentrations. TPU: thermoplastic polyurethane.

showed that the nanotube networks were well preserved even after the fabrication process with no voids.

Characterization

The tensile stress (σ) was measured as a function of tensile strain (ε'') at the rate of 0.2 mm s^{-1} at room temperature with a 50-N load cell using an Instron 5940 series tabletop testing system (TA Instruments). For the tensile measurements, we followed the ASTM D 882 standard including the testing of plastic sheets with the thickness <0.25 mm.

For thermal analysis, differential scanning calorimetry (DSC) measurements were carried out with a Q20 DSC (TA Instruments) at a heating rate of 3°C min^{-1}. Most of the measurements were collected over a temperature range of −30°C to 230°C. Thermogravimetric analysis (TGA) was carried out in atmospheric air over a temperature range of 25–800°C using a Q50 TGA (TA Instruments). The specimens were heated at a rate of 5°C min^{-1}.

For electrical conductivity measurements of the composite, copper wire leads were attached to the short ends of the rectangular composites with silver paste (DuPont 4929 N), and resistance was measured using two-probe contact direct current method with EC-Lab V10 and Fluke Ohmmeter.

Results and discussion

To study the mechanical reinforcement of the polymer (TPU) using the Baytube networks, we compare the mechanical characteristics of the composite scaffolds with up to 19 wt% nanotubes loading from measurements of tensile stress versus tensile strain at room temperature (Figure 2). The polymer (TPU) shows modulus (E) of 6.7 MPa, then plastically yielded to a more gradual deformation, followed by a steep rise in up to a stretchability of about 345% at which point the specimen broke. Modulus (E) of these composites increases dramatically with Baytube loading and reaches 1590 MPa at 19 wt% nanotube (Figure 3(a)), which corresponds to more than 20,000% improvements over that of the pristine polymer. However, stretchability decreases, and the yield point begins at a smaller strain with increasing Baytube loading. These composites did not show any sudden drop in yield. The point that is commonly observed for TPU composites[27] is due to the disintegration of the nanotube network, which demonstrates the robustness nanotube scaffold within the polymer.

Further, these composites show enhancement in UTS from 11 MPa to 30 MPa at 19 wt% nanotube loading (Figure 3(b)), which corresponds to approximately 300% improvements over that of the pristine polymer. The elongation at break of these composite scaffold decreases with CNTs loading and reaches 2.5% strain at 19 wt% nanotubes (Figure 2). The elongation at break of these composite decreases with CNT loading and reaches 2.5% strain at 19 wt% nanotubes (Figure 2).

The UTS and tensile modulus of the composites show significantly more brittle due to the stronger interfacial interactions between CNTs and polymer. These composite scaffolds with 19 wt% CNT loading showed higher modulus and UTS, higher stiffness compared to the pristine polymer due to highly packed morphology with no voids between the CNTs and the polymer. It could also be speculated that the reduction of pore size leads to more friction between the CNTs and the polymer, which leads to higher tensile strength. From the cyclic fatigue test (Figure 4), the composites scaffold aerogels show significantly higher strain hardening at 80°C than the pristine polymer. The CNTs network suppress the mobility of polymer chains and therefore the thermal motion at the interface of CNT and TPU, which lead to have a strain hardening in the elastic region (Figure 4). As the CNTs have higher surface area and mechanical properties of isotropic 3-D structure, their composite scaffold aerogels show higher mechanical characteristics.

The improved mechanical properties of these composite scaffolds might also originate from an improved structure, which can be measured using thermal stability measurements by the DSC and TGA. For the polymer, the DSC curve from the first heating cycle shows peak at $T_{m\ HS} =$ 58.8°C with an absorbed heat δH_m of 3.3 J g^{-1}, calculated from the area under the peak. This indicates that the hard segments are weakly crystalline, while the soft segments show no crystallinity (Figure 5(a)). The melting of the polymer's hard segments is reversible and shows a much weaker recrystallization on cooling at approximately 30°C. The height of the endotherm peak decreases with a loading of CNTs and becomes broader possibly due to the restricted thermal motion of the hard segments within the nanoporous nanotube networks. The restrained polymer thermal motion, which is believed to be due to an increase in the effective polymer stiffness, is likely to have contributed to the observed higher mechanical reinforcement.

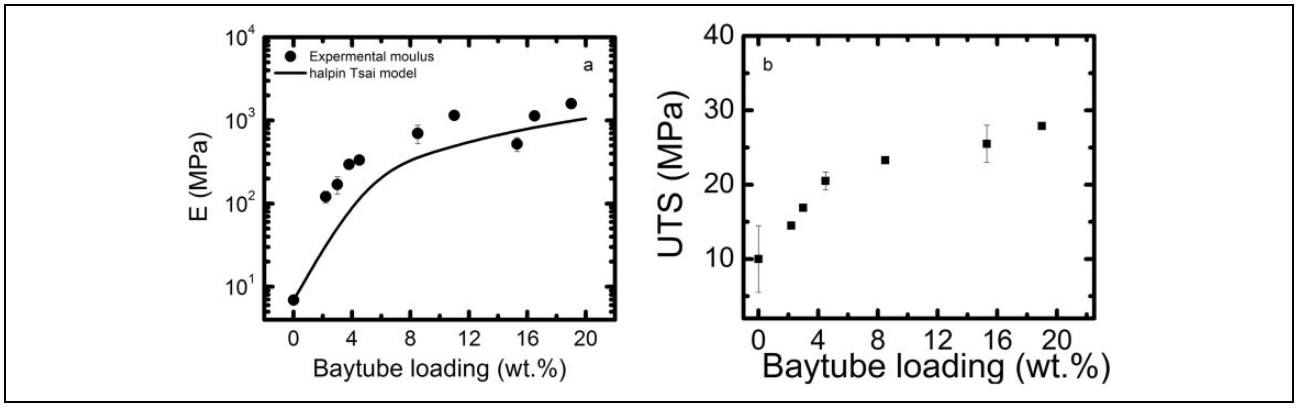

Figure 3. Mechanical characteristics of composites. (a) The values of *E* (black solid circles) of the composites increase by >20,000% with loading of 19 wt% of nanotubes. &&&The enhancement in *E* is well-predicted by the Halpin–Tsai model (block solid line). (b) The UTS of the composites (black solid square) also increases with the loading of nanotubes. The error bars are obtained from measurements on multiple samples. E: tensile modulus; UTS: ultimate tensile strength.

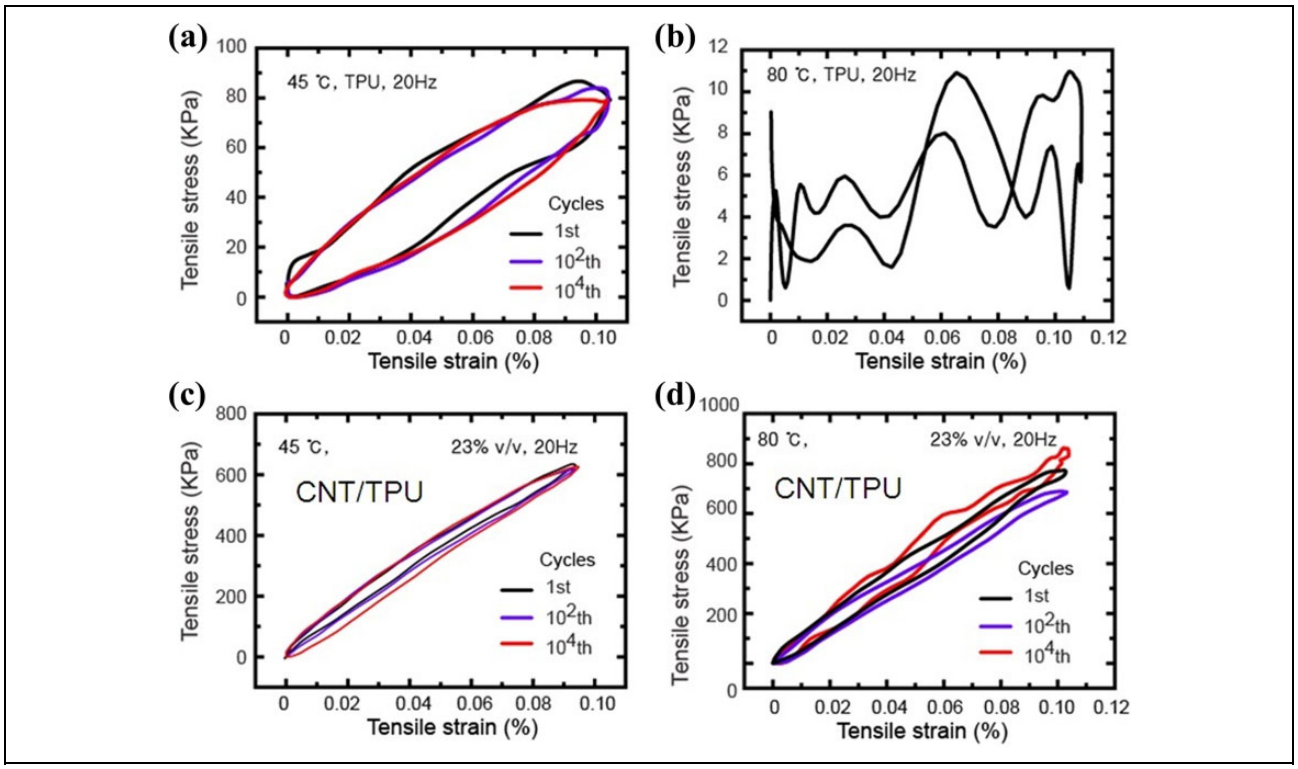

Figure 4. Cyclic fatigue test of pristine polymer TPU and composite scaffolds aerogel. TPU: thermoplastic polyurethane.

The degradation temperature of the pristine polymer is 300°C, and it shifts to a higher temperature by 40°C at 19 wt% CNTs loading. The mass loss in composite scaffolds associated with burning of polymer reduces in the presence of nanotube network because of nano-confinement. Furthermore, it shows that the degradation temperature of composite scaffold aerogels shifts to a higher temperature with increasing CNT loading. The rate of mass loss shows that degradation temperature of hard segments significantly shifts to higher temperature with an addition of nanotubes and is consistent with DSC measurements. The composites show extended thermal stability and a very slow mass loss rate when burned in the presence of atmospheric air in TGA (Figure 5(b)), and it is likely to the shift the dissociation temperature of the hard segments to a higher temperature. The nanotube network remained intact even after the composites are heated to 800°C but had a thin coating of residues, probably decomposed polymer. This higher decomposition temperature extends mechanical integrity and thermal stability of the polymer.

The intrinsic properties of individually dispersed MWCNTs may also add several beneficial features to the

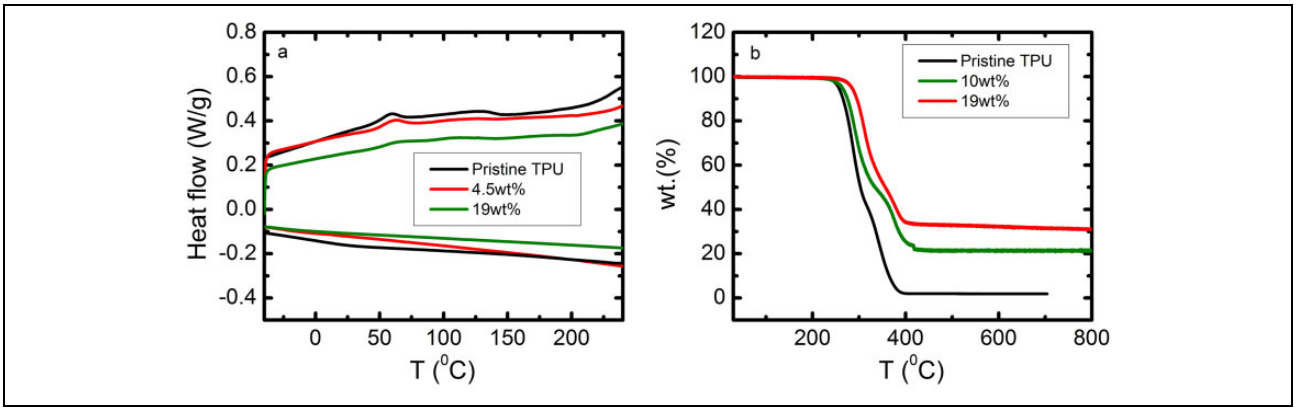

Figure 5. (a) DSC measurements of polymer and composites show reduction in polymer crystallization in the composite with increasing nanotube concentration. (b) TGA of nanotubes, polymer and composites under atmospheric air. DSC: differential scanning calorimetry; TGA: thermogravimetric analysis.

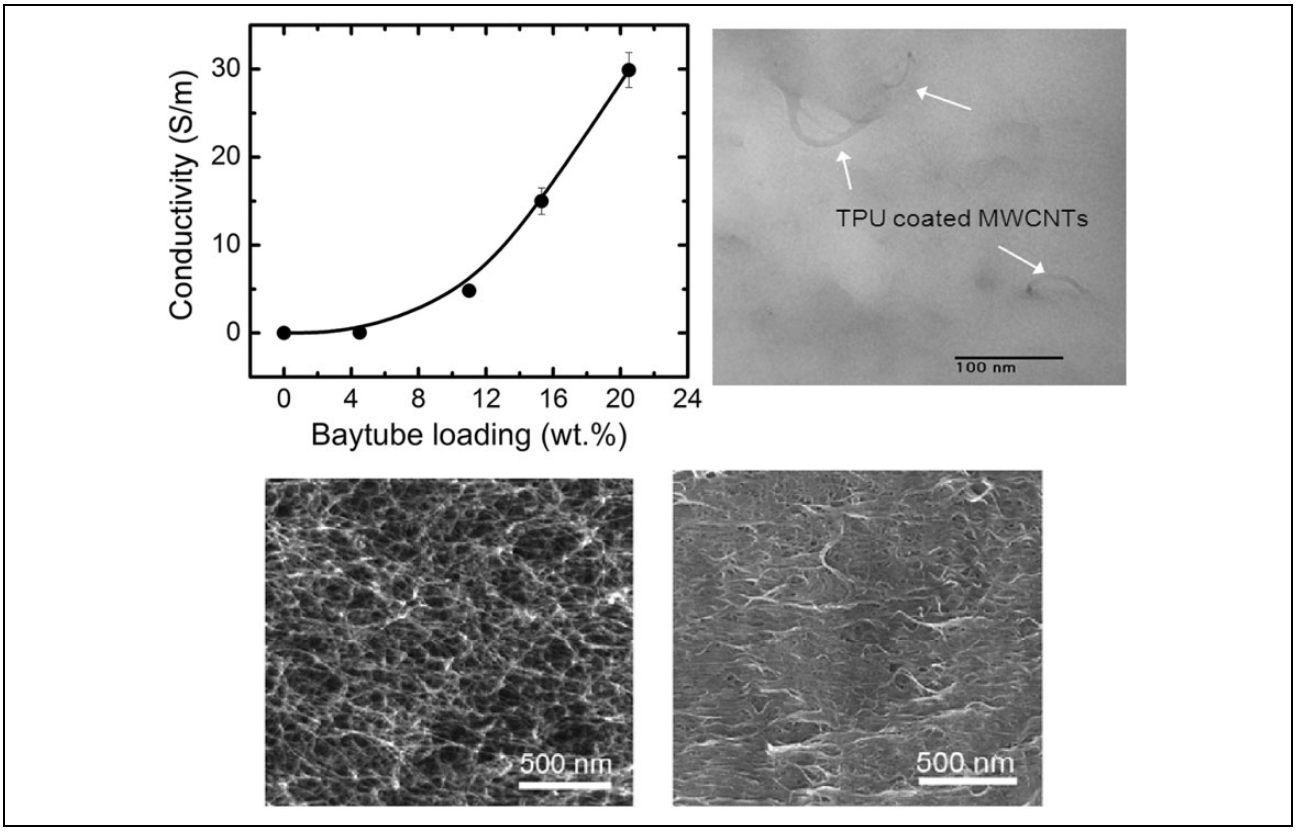

Figure 6. Electrical conductivity of aerogel-based composite scaffolds as a function of nanotubes loading (wt%) and the SEM image of CNT, TPU-coated CNTs. TPU: thermoplastic polyurethane; CNT: carbon nanotube; SEM: scanning electron microscope.

nanocomposite scaffolds. The electrical conductivity of nanocomposite scaffold aerogel increases as the function of nanotubes loading. The conductivity of the aerogel composites is higher compared to the hydrogel composites (Figure 6). It may be due to the penetration of the polymer into the nodes and degradation of the electrical contacts between the nanotubes. At lower CNT concentration, the conductivity is lower, and it might be due to less electrical contacts between the nanotube junctions. We also observe that the electrical conductivity is low at higher loading of CNTs, which might be due to higher contact resistance between the CNT junctions (Figure 6; SEM image). In these composite scaffold aerogels, larger internal surface area and stronger interfacial interaction with 3-D random network may lead to higher electrical conductivity.

Conclusion

In conclusion, we performed solution-based fabrication method to overcome the aggregation of nanotubes and improve tensile modulus about 200-fold. The nanopores of the nanotube network reduce the polymer thermal motion, resulting in the suppression of polymer glass transition and with an extension of mechanical integrity. Also, the nanotubes and polymer are thermally stable well above their degradation temperatures. Our fabrication method allows creating nanocomposites from polymers that are incompatible with nanotubes and the ones produced in this study have superior mechanical properties as well as promising smart material industrial applications.

Acknowledgments

The authors would like to acknowledge Bayer Materials for providing thermoplastic polyurethane and Baytubes.

Declaration of conflicting interests

The author(s) declared no potential conflicts of interest with respect to the research, authorship, and/or publication of this article.

Funding

The author(s) received no financial support for the research, authorship, and/or publication of this article.

ORCID iD

P Kalakonda https://orcid.org/0000-0003-1793-2069

References

1. Chung DDL. Electromagnetic interference shielding effectiveness of carbon materials. *Carbon* 2001; 39: 279–285..
2. Al-Saleh M and Sundaraj U. Electromagnetic interference (EMI) Shielding effectiveness of PP/PS polymer blends containing high structure carbon black. *Macromol Mater Eng* 2008; 293: 621–630.
3. Ci L, Suhr J, Pushparaj V, et al. Continuous carbon nanotube reinforced composites. *Nano Letter* 2008; 8: 2762–2766.
4. Bigg DM and Stutz DE. Plastic composites for electromagnetic interference shielding applications, *Polvm. Compos* 1983; 4: 40–46.
5. Rashid ESA, Ariffin K, Akil HM, et al. Mechanical and thermal properties of polymer composites for electronic packaging application. *J. Reinf. Plast. Comp* 2008; 27: 1573–1584.
6. Kharchenko SB1, Douglas JF, Obrzut J, et al. Flow-induced properties of nanotube-filled polymer materials. *Nat Mater*. August 2004; 3(8): 564–568. Epub 2004 July 25.
7. Zunfeng Liu, Gang Bai, Yi Huang, et al. Microwave absorption of single-walled carbon nanotubes/soluble cross-linked polyurethane composites. *J. Phys. Chem. C* 2007; 111(37): 13696–13700.
8. Hughes M. *Carbon Nanotube-Conducting Polymer Composites in Supercapacitors. Dekker Encyclopedia of Nanoscience and Nanotechnology*. London: Taylor & Francis, 2004, pp. 447–459.
9. Kalakonda P, Daly M, Xu K, et al. Thermal and electrical transport properties of sheared and un-sheared thin-film polymer/CNTs nanocomposites. *MRS Proc 2014* 2013; 1660: mrsf14–1660-n05–8.
10. Kalakonda P, Iannacchione GS, Daly M, et al. Calorimetric study of nanocomposites of multiwalled carbon nanotubes and isotactic polypropylene polymer. *J Appl Polym Sci* 2013; 13(1): 587–594.
11. Kalakonda P, Daly M, Xu K, et al. Structure-electrical transport property relationship of anisotropic iPP/CNT films. *MRS Proc 2013* 2013; 1499: mrsf12–1499-n05–8.
12. Kalakonda P, Gombos EA, Hoonjan GH, et al. Electrical conductivity of anisotropic iPP carbon nanotube thin films. *MRS Proc* 2012; 1410: mrsf11–1410-dd05–06.
13. Kalakonda P, Sarkar S, Gombos EA, et al. iPP/CNTs multifunctional polymer nanocomposite. *MRS Proc* 2012; 1403: mrsf11–1403-v12–13.
14. Hoefer M and Bandarua PR. Determination and enhancement of the capacitance contributions in carbon nanotube based electrode systems. *Appl. Phys. Lett* 2009; 95: 183108.
15. Halpin Affdl JC and Kardos JL. The Halpin-Tsai equations: A review. *Poly Eng Sci* 1976; 16: 344–352.
16. Breuer O and Sundararaj U. A review of polymer/carbon nanotube composites. *Polym Compos* 2004; 25: 630–645.
17. Peigney A, Laurent C, Flahaut E, et al. Specific surface area of carbon nanotubes and bundles of carbon nanotubes. *Carbon* 2001; 39: 507–514.
18. Vigolo B, Pénicaud A, Coulon C, et al. Macroscopic fibers and ribbons of oriented carbon nanotubes. *Science* 2000; 290: 1331–1334.
19. Coleman JN, Cadek M, Blake R, et al. High-performance nanotube-reinforced plastics: understanding the mechanism of strength increase. *Adv Func Mater* 2004; 14: 791–798.
20. Coleman JN, Khan U, Blau WJ, et al. Small but strong: a review of the mechanical properties of carbon nanotube-polymer composites. *Carbon* 2006; 44: 1624–1652.
21. Gui XC, Li H, Zhang L, et al. A facile route to isotropic conductive nanocomposites by direct polymer, infiltration of carbon nanotube sponges. *ACS Nano* 2011; 5: 4276–4283.
22. Zeng Y, Ci LJ, Carey BJ, et al. Design and reinforcement: vertically aligned carbon nanotube-based sandwich composites. *ACS Nano* 2010; 4: 6798–6804.
23. Hough LA, Islam MF, Hammouda B, et al. Structure of semidilute single-wall carbon nanotube suspensions and gels. *Nano Lett* 2006; 6: 313–317.
24. Bryning MB, Milkie DE, Islam MF, et al. Carbon nanotube aerogels. *Adv Mater* 2007; 19: 661–664.
25. Bryning MB, Islam MF, Kikkawa JM, et al. Very low conductivity threshold in bulk isotropic single-walled carbon nanotube–epoxy composites. *Adv Mater* 2005; 17: 1186–1191.
26. Kim KH, Oh Y and Islam MF. Graphene coating makes carbon nanotube aerogels superelastic and resistant to fatigue. *Nat Nanotech* 2012; 7: 562–566.

27. Liff SM, Kumar N and McKinley GH. High-performance elastomeric nanocomposites via solvent-exchange processing. *Nat Mater* 2007; 6: 76–83.
28. Bansal A, Yang H, Li C, et al. Quantitative equivalence between polymer nanocomposites and thin polymer films. *Nat Mater* 2005; 4: 693–698.
29. Oh H and Green PF. Polymer chain dynamics and glass transition in a thermal polymer/nanoparticle mixtures. *Nat Mater* 2009; 8: 139–143.
30. Ma WJ, Liu L, Zhang Z, et al. High-strength composite fibers: realizing true potential of carbon nanotubes in polymer matrix through continuous reticulate architecture and molecular level couplings. *Nano Lett* 2009; 9: 2855–2861.
31. Kalakonda P and Banne S. Thermomechanical properties of PMMA and modified SWCNT composites. *Nanotechnol Sci Appl* 2017; 10: 45–52.
32. Kalakonda P, Cabrera Y, Judith R, et al. Studies of electrical and thermal conductivities of sheared multi-walled carbon nanotube with isotactic polypropylene polymer composites. *Nanomater Nanotechno* 2015; 5: 2.
33. Ni C, Chattopadhyay J, Billups WE, et al. Modification of the electrical characteristics of single wall carbon nanotubes through selective functionalization. *Appl Phys lette* 2008; 93: 243113.
34. Bryning MB, Islam MF and Kikkawa JM. Very low conductivity threshold in bulk isotropic single-walled carbon nanotube-epoxy composites. *Adv Mater* 2005; 17: 1186–1191.
35. Johnston DE, Islam MF, Yodh AG, et al. Electronic devices based on purified carbon nanotubes grown by high-pressure decomposition of carbon monoxide. *Nat Mater* 2005; 4: 589–592.
36. Islam MF, Rojas E, Bergey DM, et al. High weight fraction surfactant solubilization of single-wall carbon nanotubes in water. *Nano Lett* 2003; 3: 269–273.
37. Islam MF, Milkie DE, Torrens ON, et al. Magnetic heterogeneity and alignment of single wall carbon nanotubes. *Phys Rev B* 2005; 71: 201401.
38. Hough LA, Islam MF, Janmey PA, et al. Viscoelasticity of single wall carbon nanotube suspensions. *Phys Rev Lett* 2004; 93: 168102.